CHAMP & TIE–GCM Magnetic Perturbation Comparisons

D. MOZZONI[a,c], M. MANDEA[a], AND J. CAIN[b]
[a]GeoForschungsZentrum, Potsdam, GERMANY
[b]Geophysical Fluid Dynamics Institute, Florida State University, Tallahassee, USA
[c]Department of Physics, Florida State University, Tallahassee, USA

ABSTRACT

The NCAR Thermosphere-Ionosphere Electrodynamic General Circulation Model (TIE–GCM) is a self-consistent global atmospheric model which can be used to estimate magnetic perturbations at satellite altitude. These computed perturbations can then be compared with CHAMP satellite magnetic vector data.

For the first comparison, the quietest day of each month from $2001 - 2003$ according to the list of international Q–days, was selected. CHAMP magnetic vector residuals were then computed for these intervals using the CHAOS model to remove the core and crustal geomagnetic contributions. Under various input parameters, the TIE–GCM predictions were then computed for these selected time intervals and compared with the CHAMP residuals on an orbit by orbit basis.

Initial results demonstrate a reasonable agreement between the TIE–GCM estimates and the CHAMP residuals especially in the non-polar regions ($\pm 50^o$ Latitude) where both are able to resolve the Equatorial Electro-Jet (EEJ) in the magnetic B_θ vector direction when the satellite orbit takes it near the EEJ during the January, February and September time intervals of 2002. While both show elevated activity in the polar regions, there is little consistency between the two.

1 Introduction

1.1 Introduction

The present study is an initial effort to better understand the external sources of the magnetic field hoping that it may in turn help with the development of future geomagnetic models. The Thermosphere-Ionosphere Electrodynamic General Circulation Model (TIE–GCM) is a self-consistent global atmospheric model being developed at the National Center for Atmospheric Research (NCAR) in Boulder, Colorado. This model can be used to predict many different atmospheric quantities, such as wind velocities, various atmospheric species concentrations, temperatures, electric fields, and current densities. These current densities can later be post-processed to compute magnetic perturbations both above and below the ionosphere. In order to validate these model results, one can compare the predicted perturbations calculated at the altitude of the CHAMP satellite (taken to be $430km$) with vector residuals computed from the difference of the CHAMP data and the CHAOS geomagnetic model. For this study, only the quietest day of each month was selected for this comparison. New residuals can then be computed between the original CHAMP/CHAOS residuals and estimates from the different TIE–GCM model runs for these quiet days.

1.2 Models: TIE–GCM & CHAOS

TIE–GCM: Thermosphere–Ionosphere Electrodynamic General Circulation Model (Richmond, 1992)

- A self-consistent simulation of neutral winds, conductivities, electric fields and currents.
- Below 60^o magnetic latitude the electric field is calculated by solving for the dynamo equation, while above that the electric field is imposed.
- Uses the International Geomagnetic Reference Field (IGRF) with modified magnetic apex coordinates (Richmond, 1995).
- Geomagnetic field lines are assumed to be equipotential, which reduces the electrodynamic equation to two dimensions.
- Field-aligned current flows between hemispheres so that the divergence of the total current vanishes.
- Induced Earth currents are simulated assuming a perfectly conducting layer at a depth of $600km$ below the Earth's surface.
- Height-integrated horizontal ionospheric currents are treated as currents in a thin shell at an altitude of $110km$, connected to field-aligned currents.

CHAOS: the CHAMP, Ørsted and SAC-C model of Earth's magnetic field (Olsen *et al.*, 2006)

- Spherical Harmonic Degree $n = 50$ for the static field, $n = 18$ for the first time derivative.
- Geomagnetic measurements from Ørsted, CHAMP and SAC-C taken between $03/1999 - 12/2005$ totaling over 6.5 years of high-precision geomagnetic satellite data.
- Allows for higher than usual geomagnetic activity ($K_p \leq 2$).
- Temporal variation of the core field described by splines (for $n \leq 14$).
- Uses magnetometer vector data in the instrument frame and co-estimates the Euler angles that describe the transformation from the magnetometer frame to the star imager frame, avoiding the inconsistency of using vector data that have been aligned using a different (pre-existing) field model.
- The bending of the CHAMP optical bench connecting magnetometer and star imager is accounted for by estimating Euler angles in 10 day segments.
- Co-estimates $n = 1$ external fields separately for every 12 hour interval.

1.3 Calculation of Magnetic Perturbations

Magnetic Perturbation Calculation Assumptions (Richmond, 2002)

- Height-integrated horizontal ionospheric currents are treated as currents in a thin shell located at an altitude of $110km$, connected to field-aligned currents.
- Field-aligned currents are treated as flowing on dipolar field lines, while zonal currents in the magnetosphere are ignored.
- Induced Earth currents are simulated by a perfectly conducting layer at a depth of $600km$ below the surface of the Earth.
- Calculated ground magnetic effects are used to define equivalent horizontal ionospheric currents in a shell at a height of $110km$.

Magnetic Perturbation Calculation Method

- From the TIE-GCM, a thin shell of height–integrated horizontal ionospheric current density is produced.
- The equivalent current system is then calculated, a fictitious divergence-free current sheet which produces the same magnetic perturbations at the ground.
- The equivalent current function can be expressed as an expansion in spherical harmonic coefficients (SHC).
- The SHC's are then used to calculate the magnetic potential.
- From the magnetic potential one can compute the magnetic field perturbations.

1.4 Dates Selected for Investigation

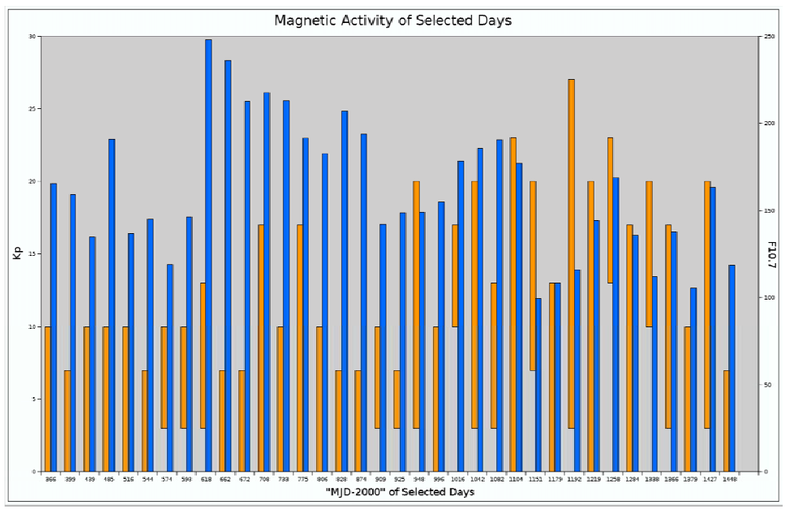

The selected dates used in this comparison study represent the quietest day of each month from $2001-2003$ as determined by the list of International Q–days. The above plot displays the corresponding activity indices K_p range (Orange) and $F10.7$ (Blue) for these days.

Date (2001)	MJD	SLT	Date (2002)	MJD	SLT	Date (2003)	MJD	SLT
Jan 01, 2001	366	11.0, 23.0	Jan 03, 2002	733	01.7, 13.7	Jan 09, 2003	1104	03.8, 15.8
Feb 03, 2001	399	08.0, 20.0	Feb 14, 2002	775	09.8, 21.8	Feb 25, 2003	1151	11.5, 23.5
Mar 15, 2001	439	04.4, 16.4	Mar 17, 2002	806	07.0, 19.0	Mar 25, 2003	1179	08.9, 20.9
Apr 30, 2001	485	00.2, 12.2	Apr 08, 2002	828	05.0, 17.0	Apr 07, 2003	1192	07.7, 19.7
May 31, 2001	516	09.3, 21.3	May 24, 2002	874	00.8, 12.8	May 04, 2003	1219	05.3, 17.3
Jun 28, 2001	544	06.8, 18.8	Jun 28, 2002	909	09.6, 21.6	Jun 12, 2003	1258	01.7, 13.7
Jul 28, 2001	574	04.1, 16.1	Jul 14, 2002	925	08.1, 20.1	Jul 08, 2003	1284	11.3, 23.3
Aug 16, 2001	593	02.4, 14.4	Aug 06, 2002	948	06.0, 18.0	Aug 31, 2003	1338	06.4, 18.4
Sep 10, 2001	618	02.0, 12.1	Sep 23, 2002	996	01.6, 13.6	Sep 28, 2003	1366	03.8, 15.8
Oct 24, 2001	662	08.1, 20.1	Oct 13, 2002	1016	11.8, 21.0	Oct 11, 2003	1379	02.6, 14.6
Nov 03, 2001	672	07.2, 19.2	Nov 08, 2002	1042	09.4, 21.4	Nov 28, 2003	1427	10.2, 22.2
Dec 09, 2001	708	03.9, 15.9	Dec 18, 2002	1082	05.7, 17.8	Dec 19, 2003	1448	08.3, 20.3

The Table lists the average Solar Local Time for the CHAMP satellite orbit passes during which the satellite was in one of the two $[-50^o, 50^o]$ latitude intervals.

2 TIE–GCM Results

2.1 Method

- The TIE–GCM was used to model each of the quiet days listed in Table 1.4.
- In order to investigate its sensitivity, the following five cases of the input $F10.7$ were used for each day:
  - $F10.7 = 70$
  - $F10.7 = 90$
  - $F10.7 = 150$
  - $F10.7 = 190$
  - $F10.7 = GPI$ – uses real-time values interpolating for every time-step (2 minutes)
- The resulting TIE–GCM output (2.2) was post-processed to compute the magnetic perturbations at satellite altitude (2.3)
- The full CHAOS model was used to compute residuals for the corresponding CHAMP vector measurements
- The TIE–GCM magnetic perturbation predictions were then compared to the CHAMP–CHAOS residuals along the orbit-track (3.1)

2.2 Height–Integrated Horizontal Current Density Maps

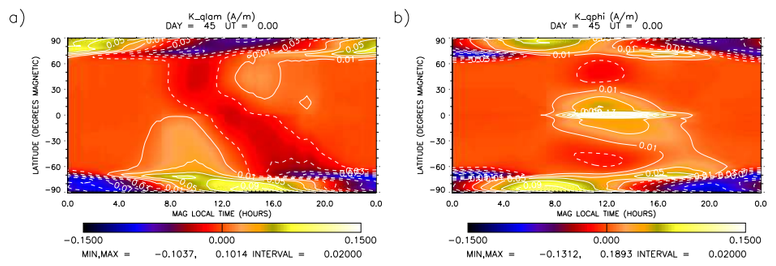

These sample plots represent the TIE–GCM predictions of the Height–Integrated Horizontal Current Density for February 14, 2002 using real-time GPI inputs rather than fixed activity index values for the Northward (a) and Eastward (b) components. The EEJ signature has been reproduced in the Eastward component.

2.3 Magnetic Perturbation Component Maps

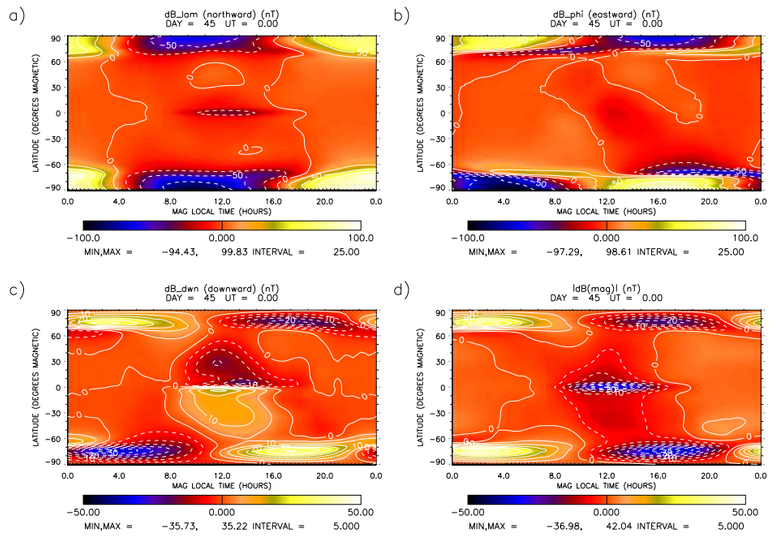

These sample plots represent the TIE–GCM predictions of the magnetic perturbation for February 14, 2002 using real-time GPI inputs rather than fixed activity index values. Plot (a) is the Northward component, (b) is the Eastward component, (c) is the Downward component, and (d) is the total field.

The EEJ signature seen in the Eastward component of the height–integrated current density produces a magnetic perturbation in the Northward magnetic perturbation component (a). The downward magnetic perturbation component (c) is associated with the Sq current system and is typified by the negative(North)/positive(South) lobe structure centered on the EEJ.

3 Comparison of Model Results

3.1 CHAMP & TIE–GCM Data with Perturbation Residuals along the Orbit Track

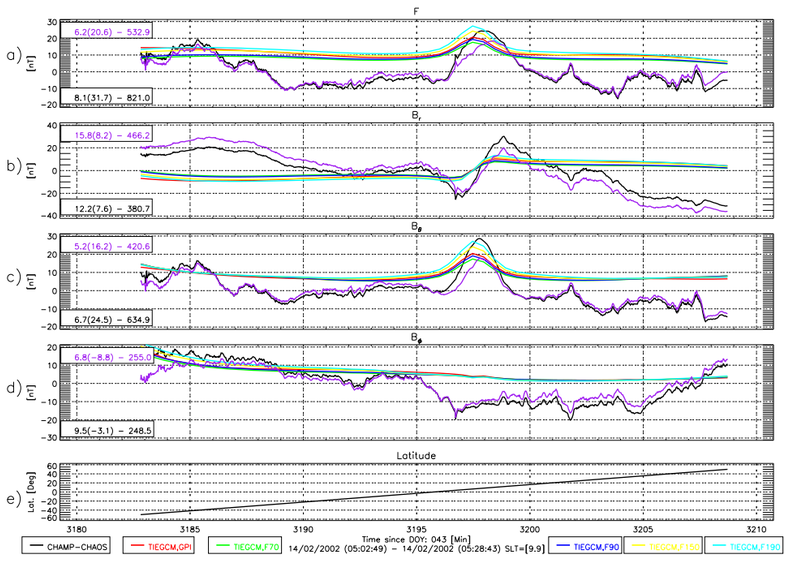

This is a plot displaying the CHAMP, TIE–GCM, and perturbation residual data along the satellite orbit track for one orbit pass on February 14, 2002 between $\pm 50^o$ latitude. The plot windows correspond to (a) the total field perturbation, (b) the B_r component of the perturbation, (c) the B_θ component, (d) the B_ϕ component, and (e) the satellite latitude.

The CHAMP/CHAOS and CHAMP/CHAOS/TIE–GCM residuals have had their mean subtracted so as to remove their offset from zero and bring all datasets to a common level. The CHAMP satellite was in approximately a 10 SLT plane.

Also plotted is a curve representing the residual calculated from the difference of the CHAMP/CHAOS residual and the predicted TIE–GCM magnetic perturbation. In the top and bottom lefthand corners, are displayed the Absolute mean deviation, Mean and Area under the curve:

[MDEV(MEAN) - AREA]

All five TIE–GCM model runs are shown vs. the CHAMP data and perturbation residuals using the following color scheme:

- $F10.7 = 70$ (GREEN)
- $F10.7 = 90$ (BLUE)
- $F10.7 = 150$ (YELLOW)
- $F10.7 = 190$ (CYAN)
- GPI (RED)
- $CHAMP/CHAOS$ Residual (BLACK)
- $CHAMP/CHAOS/TIE\text{-}GCM(GPI)$ Residual (PURPLE)

The EEJ signature in B_θ (c) for this particular orbit pass is fairly well reproduced in location, even though the amplitude is smaller. This component yields both a smaller MDEV and MEAN, likewise for total field (a). In this case the run with the $F10.7$ held fixed at 190 seems to have the best fit. (The actual $F10.7$ for this date was 191.3.

The plot window for the B_r component (b) shows the ability of the TIE–GCM to reproduce the low/high transition centered around the magnetic equator, however its poorer job in the tail region has it netting a worse overall MDEV and MEAN. The B_ϕ shows a mixed result whereby the model matched a slight trend but the amplitude was off causing a better MDEV but worse MEAN.

4 Summary of Results

4.1 Statistics of Dayside Orbit Passes for February 14, 2002

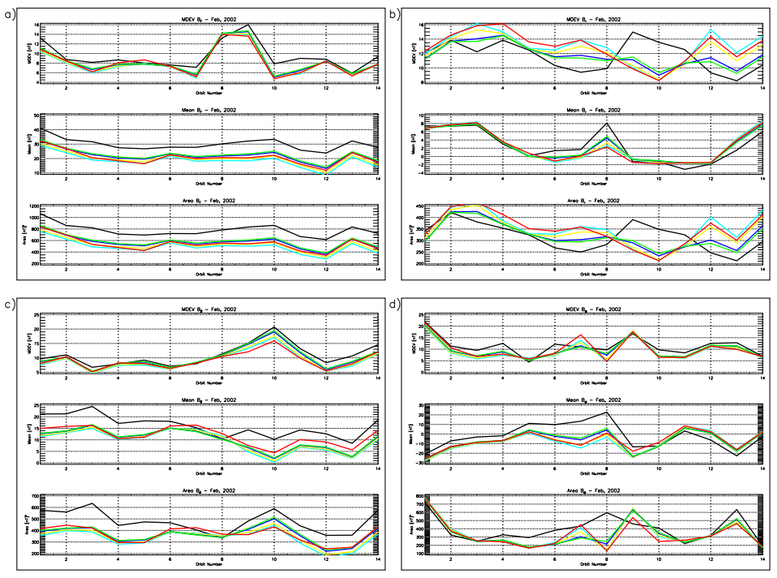

These plots show the statistics (MDEV (top), Mean (middle), and Area (bottom)) of the CHAMP/CHAOS/TIE–GCM residuals shown in section 3.1 for orbit passes on February 14, 2002 for Total field, B_F (a), B_r (b), B_θ (c), and B_ϕ (d) vs. the orbit number.

All five TIE–GCM model runs (GPI (RED), $F10.7 = 70$ (GREEN), $F10.7 = 90$ (BLUE), $F10.7 = 150$ (YELLOW), $F10.7 = 190$ (CYAN)) and the CHAMP residuals (BLACK) are displayed.

This plot actually represents a relatively good fit, whereas many individual day comparisons show more inconsistent results. In plot (a) the TIE–GCM models generally show an improvement by reducing the MDEV and Mean for the total field B_F. Likewise for the B_θ component. As is typical, the B_r and B_ϕ components are more inconsistent, varying from having a positive influence to having a negative influence.

4.2 Time-series of the Average Orbit Pass Statistics

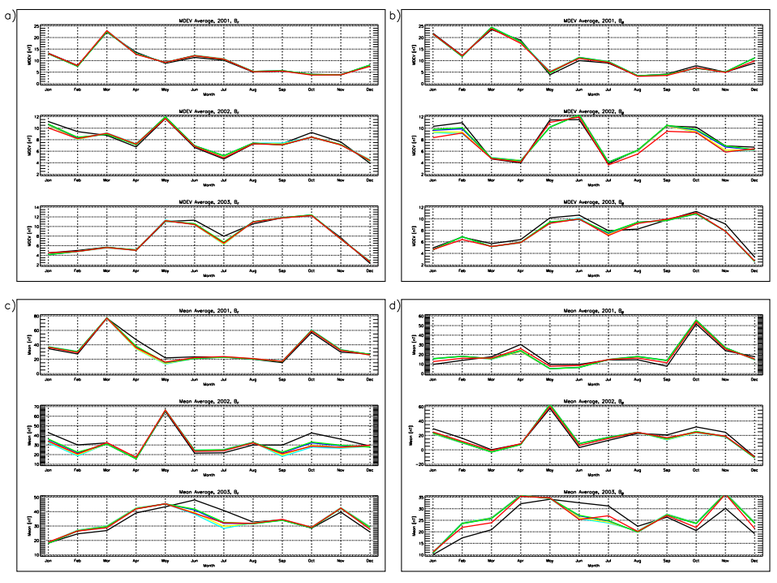

These plots show the average value of the MDEV and Mean (nT vs. Month) for each of the selected days spanning the years 2001 (top), 2000 (middle), and 2003 (bottom). The top two plots show the average MDEV for total field, B_F (a), and the B_θ component (b). While the bottom two plots show the average Mean values for the total field, B_F (c), and for the B_θ component (d).

All five TIE–GCM model runs are represented (GPI (RED), $F10.7 = 70$ (GREEN), $F10.7 = 90$ (BLUE) , $F10.7 = 150$ (YELLOW), $F10.7 = 190$ (CYAN)) as well as the CHAMP residuals (BLACK).

It is hard to draw anything conclusive, this is just an average for one day during the month after all, but overall the TIE–GCM models seem to help more then they hurt. For instance, the 2003 MDEV Average for B_θ is consistently lower than the data alone, save for the month of August.

5 Conclusions

For this study, the Thermosphere-Ionosphere Electrodynamic General Circulation Model (TIE–GCM) was used to simulate the magnetic perturbations at CHAMP satellite altitude during the quietest geomagnetically active days of each month from $2001 - 2003$. For each of these days the modeling was carried out using five different cases of the input parameter $F10.7$. The model results were then compared with residuals of vector geomagnetic field measurements computed from the difference of CHAMP data and the CHAOS geomagnetic field model.

From the above plots in the present study, one can see that the TIE–GCM can, to some degree, reproduce the residuals computed from CHAMP geomagnetic vector data. However the quality of the comparison is rather inconsistent, sometimes helpful and sometimes not. This is evidenced in the Mean average of the B_θ component for 2003 (4.2d), where there is a marked improvement from May until September, but an equally marked worsening for the other months. For that same component however, the MDEV is consistently better for the years 2002 and 2001, but not in B_F.

But overall, the fact that a model derived using no *in-situ* magnetic data can match features in satellite data at all is promising. This modeling approach better lends itself to an understanding of the physics of the ionospheric sources than would a purely parameterized model.

Clearly further study is needed to better pin-down under what conditions the model best predicts the data. To proceed in this direction it is important to expand the tested parameter space to include inputs other than just $F10.7$. These would include varying TIE–GCM inputs like the cross-tail potential, the hemispheric power, the atmospheric tides, and the electric potential model. Also broadening the selection criteria to include alternative methods of data selection like those based on the wavelet power spectrum (Schachtschneider *et al.*, 2006), or conversely to purposely include days with more elevated geomagnetic activity, should prove informative. A more robust way of quantifying the quality of fit also needs to be developed as the current method of using the MDEV and Mean statistics are insufficient and can occasionally be slightly misleading for individuals tracks.

Web Links

- CHAMP Satellite
  - http://www.gfz-potsdam.de/pb1/op/champ/
- CHAOS Geomagnetic Model
  - http://www.gfz-potsdam.de/pb2/pb23/Models/CHAOS
- International Q-days
  - http://www.gfz-potsdam.de/pb2/pb23/GeoMag/niemegk/kp_index/quietdst/
- K_p & $F10.7$ Magnetic Indices
  - http://www.gfz-potsdam.de/pb2/pb23/GeoMag/niemegk/kp_index/
- TIE–GCM
  - http://web.hao.ucar.edu/public/research/tiso/tgcm/tgcm.html

References

Olsen, N., H. Lühr, T. J. Sabaka, M. Mandea, M. Rother, L. Tøffner–Clausen, and S. Choi, CHAOS – A Model of Earth's Magnetic Field derived from CHAMP, Ørsted, and SAC–C magnetic satellite data, *Geophys. J. Int.*, in press, 2006.

Richmond, A. D., E. C. Ridley, and R. G. Roble, A Thermosphere/Ionosphere General Circulation Model with Coupled Electrodynamics, *Geophys. Res. Let.*, 19, 601–604, 1992.

Richmond, A. D., Ionospheric electrodynamics using magnetic apex coordinates, *J. Geomag. Geoelectr*, 47, 191–212, 1995.

Richmond, A. D., Modeling the geomagnetic perturbations produced by ionospheric currents, above and below the ionosphere, *J. Geodyn.*, 33, 143–156, 2002.

Schachtschneider, R., G. Balasis, M. Rother, M. Mandea, Wavelet-based selection of satellite data for geomagnetic field modelling, First Swarm International Science Meeting, Poster, May 3-5, 2006.